

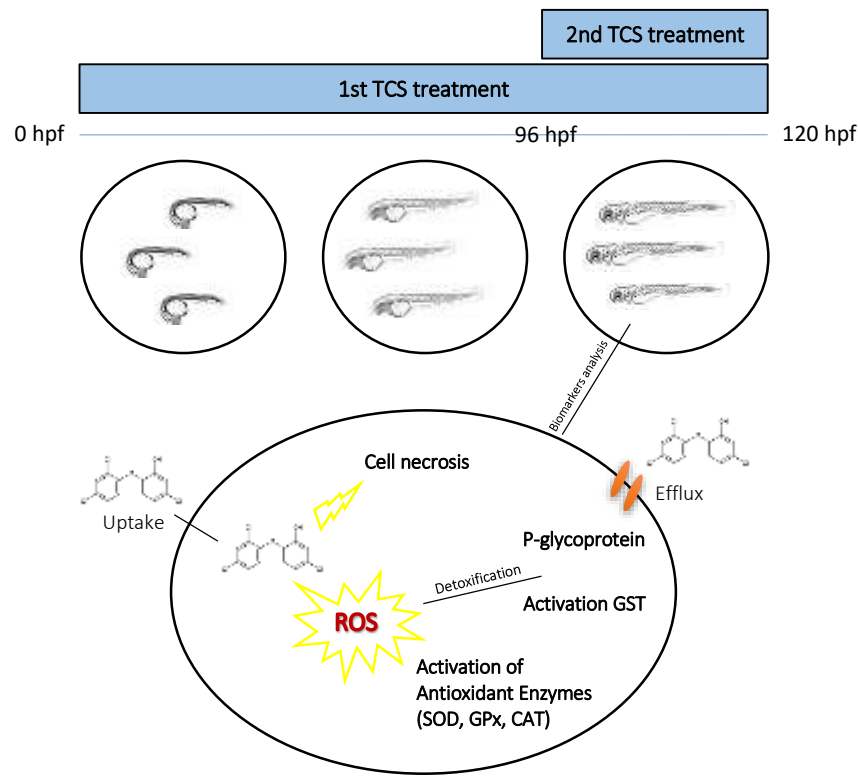
Environmental concentrations of triclosan activate cellular defence mechanism
and generate cytotoxicity on zebrafish (*Danio rerio*) embryos

Camilla Carla Parenti^{*}, Anna Ghilardi, Camilla Della Torre, Matteo Mandelli,
Stefano Magni, Luca Del Giacco, Andrea Binelli^{*}

Department of Biosciences, University of Milan, Via Celoria 26, 20133 Milan, Italy

^{*}Corresponding author e-mail: camilla.parenti@unimi.it, andrea.binelli@unimi.it

*Graphical Abstract



- TCS exposure induces P-gp efflux functionality and oxidative stress enzymes.
- Embryos cellular defence system prevent the occurrence of oxidative damage by TCS.
- High levels of cell necrosis underline TCS cytotoxicity potential.
- TCS occurrence in the aquatic environment poses an actual risk for wildlife.

Environmental concentrations of triclosan activate cellular defence mechanism
and generate cytotoxicity on zebrafish (*Danio rerio*) embryos

Camilla Carla Parenti*, Anna Ghilardi, Camilla Della Torre, Matteo Mandelli,
Stefano Magni, Luca Del Giacco, Andrea Binelli*

Department of Biosciences, University of Milan, Via Celoria 26, 20133 Milan, Italy

*Corresponding author e-mail: camilla.parenti@unimi.it, andrea.binelli@unimi.it

ABSTRACT

Triclosan (TCS, 5-chloro-2-(2,4-dichlorophenoxy) phenol) is becoming a major surface waters pollutant worldwide at concentrations ranging from ng L^{-1} to $\mu\text{g L}^{-1}$. Up to now, the adverse effects on aquatic organisms have been investigated at concentrations higher than the environmental ones, and the pathways underlying the observed toxicity are still not completely understood. Therefore, the aim of this study was to investigate the toxic effects of TCS at environmental concentrations on zebrafish embryos up to 120 hours post fertilization (hpf). The experimental design was planned considering both the quantity and the exposure time for the effects on the embryos, exposing them to two different concentrations ($0.1 \mu\text{g L}^{-1}$, $1 \mu\text{g L}^{-1}$) of TCS, for 24 hours (from 96 to 120 hpf) and for 120 hours (from 0 to 120 hpf). A suite of biomarkers was applied to measure the induction of embryos defence system, the possible increase of oxidative stress and the DNA damage. We measured the activity of glutathione-S-transferase (GST), P-glycoprotein efflux and ethoxyresorufin-o-deethylase (EROD), the level of ROS, the oxidative damage through the Protein Carbonyl Content (PCC) and the activity of antioxidant enzymes. The genetic damage was evaluated through DNA Diffusion Assay, Micronucleus test (MN test), and Comet test. The results showed a clear response of embryos defence mechanism, through the induction of P-gp efflux functionality and the activity of detoxifying/antioxidant enzymes, preventing the onset of oxidative

27 damage. Moreover, the significant increase of cell necrosis highlighted a strong cytotoxic potential
28 for TCS. The overall results obtained with environmental concentrations and both exposure time,
29 underline the critical risk associated to the presence of TCS in the aquatic environment.

30

31 1. INTRODUCTION

32 Triclosan (TCS, 5-chloro-2-(2,4-dichlorophenoxy) phenol) is an emerging contaminant included as
33 antimicrobial agent in several personal care products (PCPs), such as soaps, deodorants,
34 toothpastes, cosmetics and laundry detergents (Dann and Hontela, 2011), with a typical range of
35 0.1-0.3% of products weight (Montaseri and Forbes, 2016). The ubiquitous use of these products
36 has drawn the attention of the research community, due to the well documented TCS toxicity in
37 mammals models, including irritation of eyes and skin, allergies, detrimental effects on
38 development and reproduction, weakening of the immune system, inhibition of muscle function and
39 genotoxicity (Barbaud et al., 2005; Binelli et al., 2009; Dann and Hontela, 2011; Cherednichenko et
40 al., 2012; Savage et al., 2012; Halden, 2014). High levels of TCS were recently found in human
41 urine, blood sample, liver, adipose tissue, brain and breast milk (Ruszkiewicz et al., 2017) and its
42 structure is similar to the polychlorinated phenoxyphenols that, under oxidizing conditions, cyclize
43 to other toxic byproducts, which present very harmful effects on human health (Solá-Gutiérrez et
44 al., 2018). Furthermore, a recent proteomic study (Li et al., 2018) revealed a distinct evidence of the
45 potential impact of TCS on human metabolic pathways.

46 Nowadays, there is growing awareness for TCS environmental implications so that the marketing of
47 over-the-counter antibacterial soaps and body washes containing TCS was banned in the United
48 States since 2016 (FDA, 2016), while the European Union (EU, 2016) has disapproved the use of
49 TCS in human hygiene biocidal products (product-type 1). Nevertheless, the occurrence of TCS in
50 the aquatic ecosystems is a worldwide issue, being commonly detected in surface waters
51 (lake/river/streams with known input of raw wastewaters) with concentrations ranging from 1.4 to
52 40,000 ng L⁻¹, and in sea water from <0.001 to 100 ng L⁻¹ (Dhillon et al., 2015). There is a scientific

evidence of TCS emission from Wastewater Treatment Plants (WWTPs) into the aquatic environment, due to their partial inability to remove it, with detected concentrations ranging from 10 to 2,210 ng L⁻¹ in European WWTP effluents (Bedoux et al., 2012). TCS and mostly its methylated degradation product (methyl triclosan) are lipophilic and volatile (Wang and Kelly, 2017), causing a high tendency for bioaccumulation in aquatic organisms, which uptake them directly from food or water with bioconcentration factor (BCF) of 2.7-90 (Dhillon et al., 2015). Detected concentrations of TCS are reported in different wild organisms, such as algae and invertebrates, with concentrations up to 400 µg/kg (Coogan et al., 2008), and fish, with values up to 300 ng/g wet weight (ww) in muscle tissue (Yao et al., 2018).

The chronic and acute toxicity of TCS has been demonstrated in several aquatic models, which include green and blue algae (Orvos et al., 2002) and benthic invertebrates (Dussault et al., 2008), showing effects on biomass and growth rate, and generating oxidative stress and genotoxicity (Binelli et al., 2009; Riva et al., 2012; Martínez-Paz, 2018). In fish, TCS impacts equilibrium, swimming, spinal curvature and quiescence (Orvos et al., 2002; Ishibashi et al., 2004), as well as several studies showed the endocrine disruption effect of TCS, as demonstrated for the Japanese medaka *Oryzias latipes* (Ishibashi et al., 2004; Horie et al., 2018). Some recent studies performed on zebrafish *Danio rerio* embryos highlighted that TCS caused heart edema and slow heartbeat (Zhu et al., 2018), delayed hatching and increased mortality (Falisse et al., 2017), impaired lipid metabolism (Ho et al., 2016), and induced hepatotoxicity (Haggard et al., 2016) at concentrations up to 1.25 mg L⁻¹. Furthermore, Muth-Köhne et al. (2012) demonstrated that exposure to 3 µM TCS (870 µg L⁻¹) may have neurotoxic effects, delaying the development of zebrafish embryos motor neurons. Such results underline the TCS toxic potential for aquatic species, but do not represent a realistic scenario, since exposure concentrations are higher than those detected in aquatic ecosystems.

This study aimed to evaluate the environmental impact of TCS on aquatic ecosystem, assessing its toxic effects at environmentally relevant concentrations, and contribute to a better understanding of

the response of the organism detoxification systems to TCS exposure, using zebrafish embryos as experimental model. Embryos were exposed to two environmental concentrations (0.1 and $1 \mu\text{g L}^{-1}$) of TCS for two different exposure time, from 0 to 120 hpf and from 96 to 120 hpf, to improve the understanding on cellular detoxification mechanisms and to investigate the temporal variation of chronic toxicity in terms of oxidative stress and cyto-genotoxicity. Actually, we used a biomarker suite based on the measure of reactive oxygen species (ROS) production and the antioxidant enzymes' activity, namely catalase (CAT), superoxide dismutase (SOD) and glutathione peroxidase (GP_x). We also measured the induction of detoxification activities by the glutathione-S-transferase (GST), P-glycoprotein and ethoxyresorufin-o-deethylase (EROD), as well as the potential oxidative damage through the Protein Carbonyl Content (PCC) and cyto-genotoxic effects through the DNA Diffusion Assay, Micronucleus test (MN test) and Comet test.

2. MATERIALS AND METHODS

2.1 *Preparation of TCS solutions*

Triclosan (TCS, CAS 3380-34-5, purity 97%) was purchased from Sigma-Aldrich (Milan, Italy). Firstly, a stock solution of TCS, 1 g L^{-1} in dimethyl sulfoxide (DMSO), was prepared and stored at 4°C , while two TCS working solutions were prepared successively diluting the stock solution in ultrapure water at 0.1 mg L^{-1} and 1 mg L^{-1} , respectively. The maximum percentage of DMSO was lower than 0.0001% , and not produce any changes on hemocyte viability, DNA damage or enzyme activity (Parolini et al., 2011). These working solutions were then properly diluted to reach the selected exposure concentrations of $0.1 \mu\text{g L}^{-1}$ and $1 \mu\text{g L}^{-1}$, which fall in the range of the current environmental freshwater levels of TCS (Ho et al., 2016; Zhou et al., 2017). These concentrations also fall within the Predicted No Effect Concentration (PNEC) range (70 ng L^{-1} to $1,550 \text{ ng L}^{-1}$) reported by Capdevielle et al. (2007), which made a Species Sensitivity Distribution (SSD) analysis based on pre-existing chronic toxicity data of TCS for 14 different aquatic species.

105 2.2 Zebrafish maintenance and embryos exposure

106 Adult zebrafish of the AB strain are raised in the facility of the Department of Biosciences,
107 University of Milan, where they are maintained in tanks into a thermostatic chamber (28 °C) with
108 14-h light/10-h dark cycle. The facility follows Italian laws, rules and regulations (Legislative
109 Decree No. 116/92), as confirmed by the authorization issued by the municipality of Milan (PG
110 384983/2013).

111 Different groups of embryos were collected by means of natural spawning, following the procedure
112 for maximal embryo production described by Westerfield (2007). Control embryos were maintained
113 in zebrafish water (Instant Ocean, 0.1% methylene blue), while others were exposed to TCS (0.1 µg
114 L⁻¹ and 1 µg L⁻¹) dissolved in zebrafish water.

115 We planned two different exposures in order to evaluate the potential temporal variations, one from
116 0 hpf to 120 hpf (120 h of exposure) and the other one from 96 hpf to 120 hpf (24 h of exposure).

117 Biochemical analysis exposures were performed in 90 x 15 mm petri dish with a maximum of 70
118 embryos per petri and two replicates per experimental group, adding 25 mL of the appropriate TCS
119 working solution to each treatment group and 25 mL of zebrafish water to control groups (Fig. S1a).

120 ROS level and cyto-genotoxic biomarkers were performed in multi-well plates with 12 and 5
121 embryos per well, respectively, and three replicates per experimental group, adding 2 mL of the
122 appropriate TCS working solution to each treatment group and 2 mL of zebrafish water to control
123 groups (Fig. S1b). Both exposures (120 h and 24 h) proceeded at 28 °C under semi-static
124 conditions, replacing the exposure medium every 24 h at the longer exposure. Embryo mortality
125 and effects on morphology, developmental delay and behavioural alterations (occurrence of edema,
126 weak or no pigmentation, malformed or underdeveloped embryos, deformed spine and no or
127 malformed fins) were systematically assessed during the experiment, and no significant effects were
128 observed at chosen TCS concentrations. At the end of both exposures, embryos were processed
129 immediately for the cyto-genotoxicity endpoints or collected and stored at -80 °C until further
130 analysis.

131

132 2.3 Biochemical analysis

133 Pools of 60 embryos from each exposure was collected and homogenized, using a motorized pestle
134 mixer, in 800 μ L of 100 mM phosphate buffer (pH=7.4), with 100 mM KCl, 1 mM EDTA, 100 mM
135 dithiothreitol (DTT), and protease inhibitors (1:100 v/v). The homogenates were centrifuged at
136 12,000 r.p.m. for 10 min at 4 °C. The supernatants were collected, pooled together and immediately
137 used for the measure of glutathione-S-transferase (GST), catalase (CAT), glutathione peroxidase
138 (GPx) and superoxide dismutase (SOD) activities in triplicate, using a 6715 UV/Vis
139 spectrophotometer (Jenway, USA), following the protocol described by Della Torre et al. (2017).
140 ROS production was assessed following the method described by Parolini et al. (2017), using
141 dichlorofluorescein-diacetate (DCFH-DA). Briefly, 12 embryos from each experimental group were
142 washed with PBS and homogenized as described above. The homogenates were centrifuged at
143 15,000 r.p.m. for 20 min at 4 °C and then twenty microliters of the homogenate were added to a 96-
144 well plate and incubated for 5 min at 37 °C. We added 100 μ L of PBS and 8.3 μ L of DCFH-DA (10
145 mg/mL in DMSO) in each well before incubated the plate 30 min at 37 °C. At the end, we measured
146 the fluorescence intensity by the EnSight™ multimode plate reader (PerkinElmer) at λ_{ex} 485 nm
147 and λ_{em} 530 nm. The ROS concentration was expressed in fluorescence units (FU) mg protein⁻¹.
148 Protein carbonyl content (PCC) was measured forming protein hydrazone derivatives with 2,4-
149 dinitrophenylhydrazine (DNPH) (10 mM in 2M HCl). Proteins were then precipitated and the pellet
150 was washed and resuspended in guanidine hydrochloride (6 M). The absorbance of protein-
151 hydrazone was measured spectrophotometrically at 375 nm (Della Torre et al., 2018). A pool of
152 about 30 embryos from each exposure was used for the ethoxyresorufin-o-deethylase (EROD)
153 activity measure, which followed the same procedure described above. The EROD assay was
154 performed using the EnSight™ multimode plate reader (PerkinElmer) at λ_{ex} 535 nm and λ_{em} 590 nm
155 and temperature of 37 °C. The incubation mixture contained zebrafish embryo homogenates (4
156 replicates) in 50 mM Tris buffer pH 7.4 with BSA (5.32 mg/mL in 50 mM Tris) and NADPH (6.7

157 mM in 50 mM Tris), and the reaction substrate ethoxyresorufin (100 μ M in 15% MeOH). Standard
158 concentrations of resorufin, ranging from 0 to 0.1 μ M, were made by diluting the stock solution in
159 15% MeOH. EROD activity was calculated from the relative fluorescence units as the product of
160 resorufin, quantified with the resorufin standard curve ($R^2 = 0.99$), in $\text{pmol min}^{-1} \text{mg prot}^{-1}$. All
161 analyses were normalized on the total protein content of each sample (Table S2) measured
162 according to Bradford method using bovine serum albumin as standard (Bradford, 1976).

163

164 2.4 *Quantification of P-glycoprotein activity*

165 The efflux functionality of the P-glycoprotein (P-gp) was measured according to the procedure
166 described by Fischer et al. (2013), using Rhodamine B (RhB) as fluorescent substrate. A pool of 30
167 embryos per treatment was collected from two independent exposures and incubated for 90 minutes
168 in zebrafish water with 1 μ M RhB. For quantification of RhB uptake, embryos were homogenized
169 in 350 μ L lysis buffer (pH= 7.4) containing 10 mM KCl, 1.5 mM MgCl_2 , 10 mM Tris, and
170 centrifuged for 10 minutes at 12000 x g. One hundred μ L of the supernatant (3 replicates for each
171 treatment) were transferred to a multi-well plate and the RhB fluorescence was measured using the
172 EnSight™ multimode plate reader (PerkinElmer) at λ_{ex} 530 nm and λ_{em} 595 nm. The amount of
173 RhB was quantified with a RhB standard curve, ranging from 0 to 0.1 μ M ($R^2 = 0.99$).

174

175 2.5 *Cyto-genotoxicity*

176 Biomarkers of cyto-genotoxicity were assessed on cells obtained by mechanical dissociation as
177 described in Parolini et al. (2017), from a pool of five embryos collected from three independent
178 exposures (three pool per treatment). Cells viability was evaluated by Trypan Blue dye exclusion
179 method. The Comet assay (SCGE assay) was performed following the protocol of Kosmehl et al.
180 (2008). One hundred cells per slide (6 slides per each exposure) were analysed with the Comet
181 Score® image analysis software. DNA damage was determined by the percentage of DNA observed
182 in the comet tail and the ratio between the migration length and diameter of the comet head (LDR).

183 The same diffusion assay was used to evaluate the percentage of apoptotic/necrotic cells. Slides
184 were labelled with DAPI in order to observe DNA with a fluorescence microscope (Leica
185 DM2000). One hundred cells per slide (6 slides per each exposure) were counted, among which
186 apoptotic cells were recognized as a dense central zone surrounded by a large DNA halo, while
187 necrotic cells were visualized just as an appearance of a light DNA halo. The frequency of
188 micronuclei (MN) was evaluated on 400 cells per slide (n=9; 3 slides per pool), as reported in our
189 previous studies (Magni et al., 2016; 2017).

190

191 2.6 Statistical analysis

192 Data normality and homoscedasticity were verified using Shapiro-Wilk and Levene tests,
193 respectively. The differences between treatments and control were identified performing a one-way
194 analysis of variance (one-way ANOVA), where treatment (control, TCS 0.1 $\mu\text{g L}^{-1}$ and TCS 1 $\mu\text{g L}^{-1}$)
195 was the predictor factor, and each biomarker was a dependent variable. For both exposure times,
196 separately, the differences between treated and control were evaluated using Duncan's Multiple
197 Range *post-hoc* Test (DMRT), taking $p < 0.05$ as significant cut-off. To observe the eventual
198 covariation between tested biomarkers, we performed the Pearson's correlation considering all end-
199 points. Statistical analyses were carried out using STATISTICA 7.0 software package.

200

201 3. RESULTS AND DISCUSSION

202 Cellular response to TCS uptake was primarily evaluated through the quantification of P-gp
203 activity, which is an efflux transporter protein identified in fish and involved in detoxification
204 mechanisms, preventing the entrance of xenobiotics or eliminating them from cells (Jackson et al.,
205 2017). We observed a significantly ($F_{2,9} = 75.05$ for 24 h and $F_{2,9} = 93.39$ for 120 h; $p < 0.01$) lower
206 RhB accumulation in all treatment groups compared to the level of RhB measured in controls (Fig.
207 1a), indicating an induction of P-gp efflux functionality, probably related to active elimination of
208 TCS or its by-products from cells. Another important role in the detoxifying mechanism is due to

209 some isoforms of the cytochrome P450 superfamily, such as EROD, which catalyse the
210 transformation of several planar compounds upon the aryl hydrocarbon receptor mediated
211 regulation (Van Der Oost et al., 2003). Our results showed that TCS was not able to induce
212 significant EROD activity for both tested concentrations at the development stages analysed (Fig.
213 1b). On the other hand, the involvement of EROD activity in TCS detoxification in aquatic species
214 is still controversial, as recently described by Zhou et al. (2017), who showed the inhibition of
215 EROD upon exposure to levels of TCS up to 0.7 mg L^{-1} . Another hypothesis to explain the lack of
216 EROD modulation is related to the low inducibility of cytochrome P4501A (CYP1A) in developing
217 embryos. Indeed, a recent study in which embryos (96 hpf) were exposed to different concentrations
218 of the CYP1A inducer benzo(α)pyrene (B(α)P) showed only a low increase of *cyp1a* gene
219 transcription at the concentration of $20 \text{ } \mu\text{g L}^{-1}$ (Della Torre et al., 2017). Moreover, a previous study
220 by Saad et al. (2016), which aimed to determine the biotransformation potential of zebrafish
221 embryos during their critical window for teratogens, observed a very low CYP1A activity during
222 organogenesis. Our results seem to suggest that other enzymes (for instance CYP3A) could be
223 involved in the first phase of TCS metabolism/detoxification. The assessment of detoxification
224 activity was also evaluated through the analysis of phase II detoxifying enzyme GST, which
225 showed the same trend at the two different exposure times (Fig. 1c). The induction of GST activity
226 resulted significantly higher at the low TCS concentration ($F_{2,9} = 91.49$ and $p < 0.001$ at 24 h; $F_{2,9} =$
227 6.55 and $p < 0.01$ at 120 h). Our results are in line with findings of Oliveira et al. (2009), who
228 reported an increase of GST activity in zebrafish embryos exposed to TCS ($0.25\text{-}0.35 \text{ mg L}^{-1}$),
229 underlying the key role of GST in the detoxification response to TCS. The trend observed for GST
230 was also obtained for the activities of other antioxidant enzymes (Fig. 2a, b, c), suggesting the
231 induction of embryos antioxidant protective response upon TCS exposure. Specifically, during the
232 120 h exposure, SOD was significantly induced at $0.1 \text{ } \mu\text{g L}^{-1}$ TCS ($F_{2,9} = 10.895$; $p < 0.01$), while
233 no changes in enzymatic activity were noticed for the shorter exposure time (Fig. 2a). GPx activity
234 was again significantly induced at lower TCS concentration during both exposure times ($p < 0.01$

235 and $p < 0.05$, respectively; Fig. 2b2b). Concerning CAT, this enzyme showed a significantly higher
236 activity at lower TCS dose during the 24 h exposure ($F_{2,9} = 16.21$; $p < 0.01$; Fig. 2c), while after the
237 120 h at both tested concentrations ($F_{2,9} = 7.8609$; $p < 0.05$ and $p < 0.01$, respectively; Fig. 2c). The
238 absence of a significant modulation of detoxifying/antioxidant enzymes activity after 24 h of
239 exposure can explain the significant higher level of ROS measured at the higher TCS concentration,
240 respect to control ($F_{2,9} = 12.07$; $p < 0.01$; Fig. 2e). In the short exposure time, the first cellular
241 defence mechanism (P-gp efflux functionality) is significant activated, while the second line of
242 defence against ROS did not have enough time to be activated. On the contrary, after the longer
243 exposure time, the antioxidant enzyme activities are induced to counteract the formation of ROS
244 and restore the cellular homeostatic condition, as shown in Fig. 2e, where ROS levels are even
245 below the control (120 h exposure). In summary, our results pointed out the ability of embryos
246 cellular defence system to prevent the occurrence of oxidative damage caused by TCS exposure, as
247 it is confirmed by PCC analysis, that did not show any significant oxidative damage at all exposure
248 conditions (Fig. 2d).

249 Concerning cyto-genotoxic end-points, we verified that all treatment conditions showed a cells
250 viability higher than 90% (Table 1), a percentage well above the minimum required to perform
251 genotoxicity tests, according to the IV International Workshop on Genotoxicity Test Procedures
252 (Kirkland et al., 2007). Nevertheless, a significant decrease of cells viability was recorded in TCS $1 \mu\text{g L}^{-1}$
253 treatment after 120 h exposure ($F_{2,9} = 5.11$; $p < 0.05$). This result can be correlated to the
254 observed percentage of necrotic cells, which was significantly different from controls at the higher
255 concentration (Table 1) at both exposure times ($F_{2,9} = 21.733$ for 24 h and $F_{2,9} = 92.238$ for 120 h; p
256 < 0.001). Moreover, we also noticed a remarkable increase of necrosis at $0.1 \mu\text{g L}^{-1}$ TCS ($F_{2,9} =$
257 92.24 ; $p < 0.05$) after 120 h. The induction of cytotoxic effects by TCS was expected, since it has
258 antiseptic properties causing cell lysis by lipid, RNA and protein synthesis inhibition, and
259 membrane perturbations (Schweizer, 2001). The biomarkers of genotoxicity (SCGE assay and MN
260 test) revealed that exposures to environmental concentrations of TCS induced only low genotoxic

effects in zebrafish embryos. The primary genetic damage measured by the SCGE assay was evaluated both through the percentage of DNA tail and the LDR. Although both of them mostly remained within the physiological range, the percentage of DNA tail showed a significant ($F_{2,9} = 29.32$; $p < 0.01$) frequency of DNA damage at the end of the 120 h exposure, revealing a slight primary genotoxic effect caused by the higher TCS concentration (Table 1). The mild level of genotoxicity was confirmed by the lack of chromosomal damage, highlighted by the MN test, that showed no significant differences between treatments and control during both exposure tests (Table 1). This result seems to be in contrast with the high MN frequency observed in zebra mussel specimens exposed to TCS (Binelli et al., 2009), although the previous studies tested concentrations were at least three times higher than those used in this study. The low genetic damage observed might be correlated to embryos high resistance to the genotoxic injury, as well to the short time of exposure, in agreement with a previous study (Della Torre et al., 2017) in which zebrafish embryos exposed to the carcinogen B(α)P up to 96 hpf did not show any significant induction of primary DNA damage and occurrence of MN. The overall results obtained by both biochemical and cytogenotoxicity analyses suggest that the observed cyto-genotoxic effects were produced directly by TCS and not indirectly related to an increase of oxidative stress.

Finally, all the investigated endpoints were combined together to evaluate their relationship through the Pearson's correlation statistic test (Table 2). The positive significant correlation between GST and antioxidant enzymes suggests that also this enzyme is actively involved in preventing oxidative stress, as also supported by the negative significant correlation with ROS level. These results are similar to those reported for the catfish *Pelteobagrus fulvidraco* (Ku et al., 2014), in which TCS exposure induced a significant increase of CAT activity, and for zebra mussel that showed a rise of GST and CAT activities in response to TCS (Binelli et al., 2011). The positive correlation highlighted between SOD and GPx (Table 2; Fig. S3), but not with CAT, confirmed the slight oxidative stress generated by environmental concentrations of TCS. Indeed, GPx is more sensitive to low H₂O₂ concentrations generated by SOD, while CAT is induced only by high levels of this

oxidative by-product (Powers and Lennon, 1999). Lastly, the cell viability was negatively correlated ($p < 0.01$) with necrosis suggesting the independent cytotoxic effect of environmental levels of TCS on zebrafish embryos.

290

291 CONCLUSIONS

This study is the first attempt to investigate the potential toxicity of TCS administered at environmental concentrations on zebrafish embryos. TCS exposure elicited the induction of oxidative stress response in embryos, preventing the occurrence of oxidative damage. Though, the pollutant generated a significant cytotoxicity, which subsequently drives to an increase of cellular necrosis.

Overall results highlight the concern related to the presence of TCS in the aquatic environment, suggesting the need to assess the effective exposure of aquatic wildlife to this pollutant. Further studies focusing on understanding the toxicity mechanisms of TCS on other aquatic models and including the investigation of other endpoints (i.e. transcription levels of stress related genes, proteomics) at environmental concentrations are also recommended.

302

303 REFERENCES

Andersson, T. and Förlin, L., 1992. Regulation of the cytochrome P450 enzyme system in fish. *Aquat. Toxicol.* 24, 1-19.

306

Barbaud, A., Vigan, M., Delrous, J.L., Assier, H., Avenel-Audran, M., Collet, E., Dehlemmes, A., Dutartre, H., Geraut, C., Girardin, P., Le Coz, C., Milpied-Homsi, B., Nassif, A., Pons-Guiraud A., Raison-Peyron, N., Membres du Groupe du, R., 2005. Contact allergy to antiseptics: 75 cases analyzed by the dermato-allergovigilance network (Revidal). *Ann. Dermatol. Venereol.* 132 (12 Pt. 1), 962-965.

312

313 Bedoux, G., Roig, B., Thomas, O., Dupont, V., Le Bot, B., 2012. Occurrence and toxicity of
314 antimicrobial triclosan and by-products in the environment. *Environ. Sci. Pollut. Res.* 19, 1044-
315 1065.

316

317 Binelli, A., Cogni, D., Parolini, M., Riva, C., Provini, A., 2009. *In vivo* experiments for the
318 evaluation of genotoxic and cytotoxic effects of Triclosan in Zebra mussel hemocytes. *Aquat.*
319 *Toxicol.* 91, 238-244.

320

321 Binelli, A., Parolini, M., Pedriali, A., Provini, A., 2011. Antioxidant Activity in the Zebra Mussel
322 (*Dreissena polymorpha*) in Response to Triclosan Exposure. *Water Air Soil Pollut.* 217, 421-
323 430.

324

325 Bradford, M.M., 1976. A rapid and sensitive method for the quantification of microgram quantities
326 of protein using the principle of protein-dye binding. *Anal. Biochem.*, 72, 248-254.

327

328 Capdevielle, M., Van Egmond, R., Whelan, M., Versteeg, D., Hofmann-Kamensky, M., Inauen, J.,
329 Cunningham, V., Woltering, D., 2007. Consideration of exposure and species sensitivity of
330 Triclosan in the freshwater environment. *Integr. Environ. Assess. Manag.* 4 (1), 15-23.

331

332 Cherednichenko, G., Zhang, R., Bannister, R.A., Timofeyev, V., Li, N., Fritsch, E.B., Feng, W.,
333 Barrientos, G.C., Schebb, N.H., Hammock, B.D., Beam, K.G., Chiamvimonvat, N., Pessah, I.N.,
334 2012. Triclosan impairs excitation-contraction coupling and Ca^{2+} dynamics in striated muscle.
335 *Proc. Natl. Acad. Sci. U.S.A.* 109 (35), 14158-14163.

336

337 Coogan, M.A. and La Point, T.W., 2008. Snail bioaccumulation of triclocarban, triclosan and
 338 methyltriclosan in a north Texas, USA, stream affected by wastewater treatment plant runoff.
 339 Environ. Toxicol. Chem. 27, No. 8, 1788-1793.

340

341 Dann, A.B. and Hontela, A., 2011. Triclosan: environmental exposure, toxicity and mechanisms of
 342 action. J. Appl. Toxicol. 31, 285-311.

343

344 Della Torre, C., Maggioni, D., Ghilardi, A., Parolini, M., Santo, N., Landi, C., Madaschi, L., Magni,
 345 S., Tasselli, S., Ascagni, M., Bini, L., La Porta, C., Del Giacco, L., Binelli, A., 2018. The
 346 interactions of fullerene C₆₀ and Benzo(α)pyrene influence their bioavailability and toxicity to
 347 zebrafish embryos. Environ. Pollut. 241, 999-1008.

348

349 Della Torre, C., Parolini, M., Del Giacco, L., Ghilardi, A., Ascagni, M., Santo, N., Maggioni, D.,
 350 Magni, S., Madaschi, L., Prosperi, L., La Porta, C., Binelli, A., 2017. Adsorption of B(α)P on
 351 carbon nanopowder affects accumulation and toxicity in zebrafish (*Danio rerio*) embryos.
 352 Environ. Sci.: Nano 4, 1132-1146.

353

354 Dhillon, G.S., Kaur, S., Pulicharla, R., Brar, S.K., Cledón, M., Verma, M., Surampalli, R.Y., 2015.
 355 Triclosan: Current Status, Occurrence, Environmental Risks and Bioaccumulation Potential. Int.
 356 J. Environ. Res. Public Health 12, 5657-5684.

357

358 Dussault, È.B., Balakrishnan, V.K., Sverko, E., Solomon, K.R., Sibley, P.K., 2008. Toxicity of
 359 human pharmaceutical and personal care products to benthic invertebrates. Environ. Toxicol.
 360 Chem. 27, No. 2, 435-442.

361

362 EU, 2016. Commission implementing decision (EU) 2016/110: Not approving triclosan as an
 363 existing active substance for use in biocidal products for product type1.
 364 <http://www.eufram.com/documents/EUFRAM%20WP5%20draft%20report%202005.pdf>.
 365 Accessed 11 Aug 2016.
 366

367 Falisse, E., Voisin, A., Silvestre, F., 2017. Impacts of triclosan exposure on zebrafish early-life
 368 stage: Toxicity and acclimation mechanisms. *Aquat. Toxicol.* 189, 97-107.
 369

370 FDA, 2016. FDA issues final rule on safety and effectiveness of antibacterial soaps.
 371 <https://www.fda.gov/NewsEvents/Newsroom/PressAnnouncements/ucm517478.htm>. Accessed 2
 372 Oct 2016.
 373

374 Fischer, S., Klüver, N., Burkhardt-Medicke, K., Pietsch, M., Schmidt, A., Wellner, P., Schirmer, K.,
 375 Luckenbach, T., 2013. Abcb4 acts as multixenobiotic transporter and active barrier against
 376 chemical uptake in zebrafish (*Danio rerio*) embryos. *BMC Biology* 11:69.
 377

378 Haggard, D.E., Noyes, P.D., Waters, K.M., Tanguay, R.L., 2016. Phenotypically anchored
 379 transcriptome profiling of developmental exposure to the antimicrobial agent, triclosan, reveals
 380 hepatotoxicity in embryonic zebrafish. *Toxicol. Appl. Pharmacol.* 308, 32-45.
 381

382 Halden, R.U., 2014. On the Need and Speed of Regulating Triclosan and Triclocarban in the United
 383 States. *Environ. Sci. Technol.* 48 (7), 3603-3611.
 384

385 Ho, J.C.H., Hsiao, C.D., Kawakami, K., Tse, W.K.F., 2016. Triclosan (TCS) exposure impairs lipid
 386 metabolism in zebrafish embryos. *Aquat. Toxicol.* 173, 29-35.
 387

388 Horie, Y., Yamagishi, T., Takahashi, H., Iguchi, T., Tatarazako, N., 2018. Effects of triclosan on
389 Japanese medaka (*Oryzias latipes*) during embryo development, early life stage and
390 reproduction. J. Appl. Toxicol. 38, 544-551.

391

392 Ishibashi, H., Matsumura, N., Hirano, M., Matsuoka, M., Shiratsuchi, H., Ishibashi, Y., Takao, Y.,
393 Arizono, K., 2004. Effects of triclosan on the early life stages and reproduction of medaka
394 *Oryzias latipes* and induction of hepatic vitellogenin. Aquat. Toxicol. 67, 167-179.

395

396 Jackson, J.S., Kennedy, C.J., 2017. Regulation of hepatic *abcb4* and *cyp3a65* gene expression and
397 multidrug/multixenobiotic resistance (MDR/MXR) functional activity in the model teleost,
398 *Danio rerio* (zebrafish). Comp. Biochem. Physiol. C, 200, 34-41.

399

400 Kirkland, D., Pfuhler, S., Tweats, D., Aardema, M., Corvi, R., Darroudi, F., Elhajouji, A., Glatt, H.,
401 Hastwell, P., Hayashi, M., Kiasper, P., Kirchner, S., Lynch, A., Marziu, D., Maurice, D.,
402 Meunier, J.R., Muller, L., Nohynek, G., Parry, E., Thybaud, V., Tice, R., Van Benthem, J.,
403 Vanparys, P., White, P., 2007. How to reduce false positive results when undertaking in vitro
404 genotoxicity testing and thus avoid unnecessary follow-up animal tests. Report of an ECVAM
405 Workshop. Mutat. Res. 628, 31-55.

406

407 Kosmehl, T., Hallare, A.V., Braunbeck, T., Hollert, H., 2008. DNA damage induced by
408 genotoxicants in zebrafish (*Danio rerio*) embryos after contact exposure to freeze-dried sediment
409 and sediment extracts from laguna lake (The Philippines) as measured by the comet assay.
410 Mutat. Res. 650, 1-14.

411

412 Ku, P., Wu, X., Nie, X., Ou, R., Wang, L., Su, T., Li, Y., 2014. Effects of triclosan on the
413 detoxification system in the yellow catfish (*Pelteobagrus fulvidraco*): Expression of CYP and

414 *GST* genes and corresponding enzyme activity in phase I, II and antioxidant system. Comp.
 415 Biochem. Physiol. C, 166, 105-114.

416

417 Li, Y., Li, C., Qin, H., Yang, M., Ye, J., Long, Y., Ou, H., 2018. Proteome and phospholipid
 418 alteration reveal metabolic network of *Bacillus thuringiensis* under triclosan stress. Sci. Total
 419 Environ. 615, 508-516.

420

421 Magni, S., Parolini, M., Binelli, A., 2016. Sublethal effects induced by morphine to the freshwater
 422 biological model *Dreissena polymorpha*. Environ. Toxicol. 31, 58-67.

423

424 Magni, S., Parolini, M., Della Torre, C., Fernandes de Oliveira, L., Catani, M., Guzzinati, R.,
 425 Cavazzini, A., Binelli, A., 2017. Multi-biomarker investigation to assess toxicity induced by two
 426 antidepressants on *Dreissena polymorpha*. Sci. Total Environ. 578, 452-459.

427

428 Martínez-Paz, P., 2018. Response of detoxification system genes on *Chironomus riparius* aquatic
 429 larvae after antibacterial agent triclosan exposures. Sci. Total Environ. 624, 1-8.

430

431 Montaseri, H., Forbes, P.B.C., 2016. A review of monitoring methods for triclosan and its
 432 occurrence in aquatic environments. Trends Anal. Chem. 85, 221-231.

433

434 Muth-Köhne, E., Wichmann, A., Delov, V., Fenske, M., 2012. The classification of motor neuron
 435 defects in the zebrafish embryo toxicity test (ZFET) as an animal alternative approach to assess
 436 developmental neurotoxicity. Neurotoxicol. Teratol. 34, 413-424.

437

438 Oliveira, R., Domingues, I., Grisolia, C.K., Soares, A.M.V.M., 2009. Effects of triclosan on
 439 zebrafish early-life stages and adults. Environ. Sci. Pollut. Res. 16, 679-688.

440
441
442
443
444
445
446
447
448
449
450
451
452
453
454
455
456
457
458
459
460
461
462
463
464
465

Orvos, D.R., Versteeg D.J., Inauen, J., Capdevielle, M., Rothenstein, A., Cunningham, V., 2002. Aquatic toxicity of triclosan. *Environ. Toxicol. Chem.* 21, No. 7, 1338-1349.

Parolini, M., Binelli, A., Provini, A., 2011. Assessment of the Potential Cyto-Genotoxicity of the Nonsteroidal Anti-Inflammatory Drug (NSAID) Diclofenac on the Zebra Mussel (*Dreissena polymorpha*). *Water Air Soil Pollut.* 217, 589-601.

Parolini, M., Ghilardi, A., Della Torre, C., Magni, S., Prosperi, L., Calvagno, M., Del Giacco, L., Binelli, A., 2017. Environmental concentrations of cocaine and its main metabolites modulated antioxidant response and caused cyto-genotoxic effects in zebrafish embryo cells. *Environ. Pollut.* 226, 504-514.

Powers, S.K., Lennon, S.L., 1999. Analysis of cellular responses to free radicals: Focus on exercise and skeletal muscle. *Proc. Nutr.* 58, 1025-1033.

Ramaswamy, B.R., Shanmugam, G., Velu, G., Rengarajan, B., Larsson, D.G.J., 2011. GC–MS analysis and ecotoxicological risk assessment of triclosan, carbamazepine and parabens in Indian rivers. *J. Hazard. Mater.* 186, 1586-1593.

Riva, C., Cristoni, S., Binelli, A., 2012. Effects of triclosan in the freshwater mussel *Dreissena polymorpha*: A proteomic investigation. *Aquat. Toxicol.* 118-119, 62-71.

Ruszkiewicz, J.A., Shaojun, L., Rodriguez, M.B., Aschner, M., 2017. Is Triclosan a neurotoxic agent? *J. Toxicol. Environ. Health. Part B*, 20:2, 104-117.

466 Saad, M., Verbueken, E., Pype, C., Casteleyn, C., Van Ginneken, C., Maes, L., Cos, P., Van
 467 Cruchten, S., 2016. *In vitro* CYP1A activity in the zebrafish: temporal but low metabolite levels
 468 during organogenesis and lack of gender differences in the adult stage. *Reprod. Toxicol.* 64, 50-
 469 56.
 470
 471 Savage, J.H., Matsui, E.C., Wood, R.A., Keet, C.A., 2012. Urinary levels of triclosan and parabens
 472 are associated with aeroallergen and food sensitization. *J. Allergy Clin. Immunol.* 130 (2), 453-
 473 460 e7.
 474
 475 Schweizer, H.P., 2001. Triclosan: a widely used biocide and its link to antibiotics. *FEMS*
 476 *Microbiol. Letters* 202, 1-7.
 477
 478 Solá-Gutiérrez, C., San Román, M.F. and Ortiz, I., 2018. Fate and hazard of the electrochemical
 479 oxidation of triclosan. Evaluation of polychlorodibenzo p dioxins and polychlorodibenzofurans
 480 (PCDD/Fs) formation. *Sci. Total Environ.* 626, 126-133.
 481
 482 Van der Oost, R., Beyer, J., Vermeulen, N.P.E., 2003. Fish bioaccumulation and biomarkers in
 483 environmental risk assessment: a review. *Environ. Toxicol. Pharmacol.* 13, 57-149.
 484
 485 Wang, Q. and Kelly, B.C., 2017. Occurrence and distribution of synthetic musks, triclosan and
 486 methyl triclosan in a tropical urban catchment: influence of land-use proximity, rainfall and
 487 physicochemical properties. *Sci. Total Environ.* 574, 1439-1447.
 488
 489 Westerfield, M., 2007. *THE ZEBRAFISH BOOK*, 5th Edition. A guide for the laboratory use of
 490 zebrafish (*Danio rerio*), Eugene, University of Oregon Press. Paperback.
 491

492 Yao, L., Zhao, J., Liu, Y., Zhang, Q., Jiang, Y., Liu, S., Liu, W., Yang, Y., Ying, G., 2018. Personal
493 care products in wild fish in two main Chinese rivers: Bioaccumulation potential and human
494 health risks. *Sci. Total Environ.* 621, 1093-1102.

495

496 Zhou, Z., Yang, J., Chan, K.M., 2017. Toxic effects of triclosan on a zebrafish (*Danio rerio*) liver
497 cell line, ZFL. *Aquat. Toxicol.* 191, 175-188.

498

499 Zhu, L., Shao, Y., Xiao, H., Santiago-Schübel, B., Meyer-Alert, H., Schiwy, S., Yin, D., Hollert, H.
500 and Küppers, S., 2018. Electrochemical simulation of triclosan metabolism and toxicological
501 evaluation. *Sci. Total Environ.* 622, 1193-1201.

502

503 FIGURE CAPTIONS

504 *Fig. 1.* Activity of P-glycoprotein (a), EROD (b) and GST (c) in zebrafish embryos exposed for 24 h and 120 h to TCS at
505 $0.1 \mu\text{g L}^{-1}$ and $1 \mu\text{g L}^{-1}$, compared to relative control (mean \pm SD).

506 One-way ANOVA, Duncan's Multiple Range post-hoc test, $**p < 0.01$, $***p < 0.001$.

507

508 *Fig. 2.* Activity levels of antioxidant enzymes (SOD, GPx and CAT) in zebrafish embryos exposed for 24 h and 120 h to
509 TCS at $0.1 \mu\text{g L}^{-1}$ and $1 \mu\text{g L}^{-1}$, compared to relative controls (mean \pm SD).

510 One-way ANOVA, Duncan's Multiple Range post-hoc test, $*p < 0.05$, $**p < 0.01$.

Table 1. Biomarkers of cyto-genotoxicity in zebrafish exposed for 24 h and 120 h to TCS at 0.1 µg L⁻¹ and 1 µg L⁻¹ (mean ± SD). One-way ANOVA, Duncan’s Multiple Range post-hoc test, *p < 0.05, **p < 0.01, ***p < 0.001.

TREATMENT	CELL VIABILITY (%)	DNA TAIL (%)	LDR (%)	NECROSIS (%)	MICRONUCLEI (‰)
24 h					
ctrl	96.94 ± 0.52	1.92 ± 0.49	1.03 ± 0.01	2.37 ± 0.93	3.61 ± 1.16
0.1 µg L ⁻¹	97.18 ± 1.27	1.87 ± 0.39	1.03 ± 0.00	1.91 ± 0.71	4.45 ± 0.73
1 µg L ⁻¹	95.19 ± 3.77	1.55 ± 0.49	1.03 ± 0.01	***5.76 ± 1.22	5.40 ± 2.49
120 h					
ctrl	98.70 ± 1.33	2.07 ± 0.20	1.03 ± 0.00	0.90 ± 0.74	5.03 ± 2.78
0.1 µg L ⁻¹	97.16 ± 2.66	*1.43 ± 0.39	1.02 ± 0.01	*3.61 ± 1.22	7.25 ± 2.04
1 µg L ⁻¹	*94.69 ± 2.36	**2.80 ± 0.34	1.04 ± 0.00	***12.83 ± 2.28	9.51 ± 7.39

Table 2. Matrix of Pearson’s correlation, showing r and p-level, for all biomarkers examined in zebrafish exposed for 24 h and 120 h to TCS at 0.1 µg L⁻¹ and 1 µg L⁻¹. Significant correlations (p < 0.05) are reported in bold.

	GST	CAT	GPx	SOD	P-gp	EROD	MN	VIAB	NECRO	COMET	PCC	ROS
GST	1.0000	0.8028 p=0.000	0.6000 p=0.003	0.4428 p=0.039	-0.3059 p=0.166	0.4078 p=0.060	0.2069 p=0.355	0.1975 p=0.378	0.0093 p=0.967	0.1135 p=0.615	0.3700 p=0.090	-0.5425 p=0.009
CAT		1.0000	0.5988 p=0.003	0.2084 p=0.352	-0.2091 p=0.350	0.3875 p=0.075	0.3761 p=0.085	0.0223 p=0.921	0.3072 p=0.164	0.2782 p=0.21	-0.1322 p=0.557	-0.4991 p=0.018
GPx			1.0000	0.5134 p=0.015	0.1423 p=0.528	0.8040 p=0.000	0.4211 p=0.051	0.1339 p=0.552	0.2523 p=0.257	0.2642 p=0.235	-0.4003 p=0.065	-0.7595 p=0.000
SOD				1.0000	-0.4429 p=0.039	0.4839 p=0.023	0.1515 p=0.501	0.1527 p=0.498	-0.1501 p=0.505	-0.3685 p=0.092	-0.6590 p=0.001	-0.3667 p=0.093
P-gp					1.0000	0.0218 p=0.923	-0.2057 p=0.358	0.2084 p=0.352	-0.0226 p=0.920	0.4904 p=0.02	0.2748 p=0.216	-0.1732 p=0.441
EROD						1.0000	0.4904 p=0.020	-0.0211 p=0.926	0.1501 p=0.505	0.1516 p=0.501	-0.3429 p=0.118	-0.6262 p=0.002
MN							1.0000	0.0694 p=0.759	0.0736 p=0.745	-0.2301 p=0.303	0.1678 p=0.455	-0.2041 p=0.362
VIAB								1.0000	-0.6239 p=0.002	-0.0537 p=0.812	0.2747 p=0.216	0.0962 p=0.0670
NECRO									1.0000	0.6020 p=0.003	-0.3295 p=0.134	-0.3709 p=0.089
COMET										1.0000	-0.0553 p=0.807	-0.3663 p=0.094
PCC											1.0000	0.5256 p=0.012

Figure
Click here to download Figure: Fig. 1.pdf

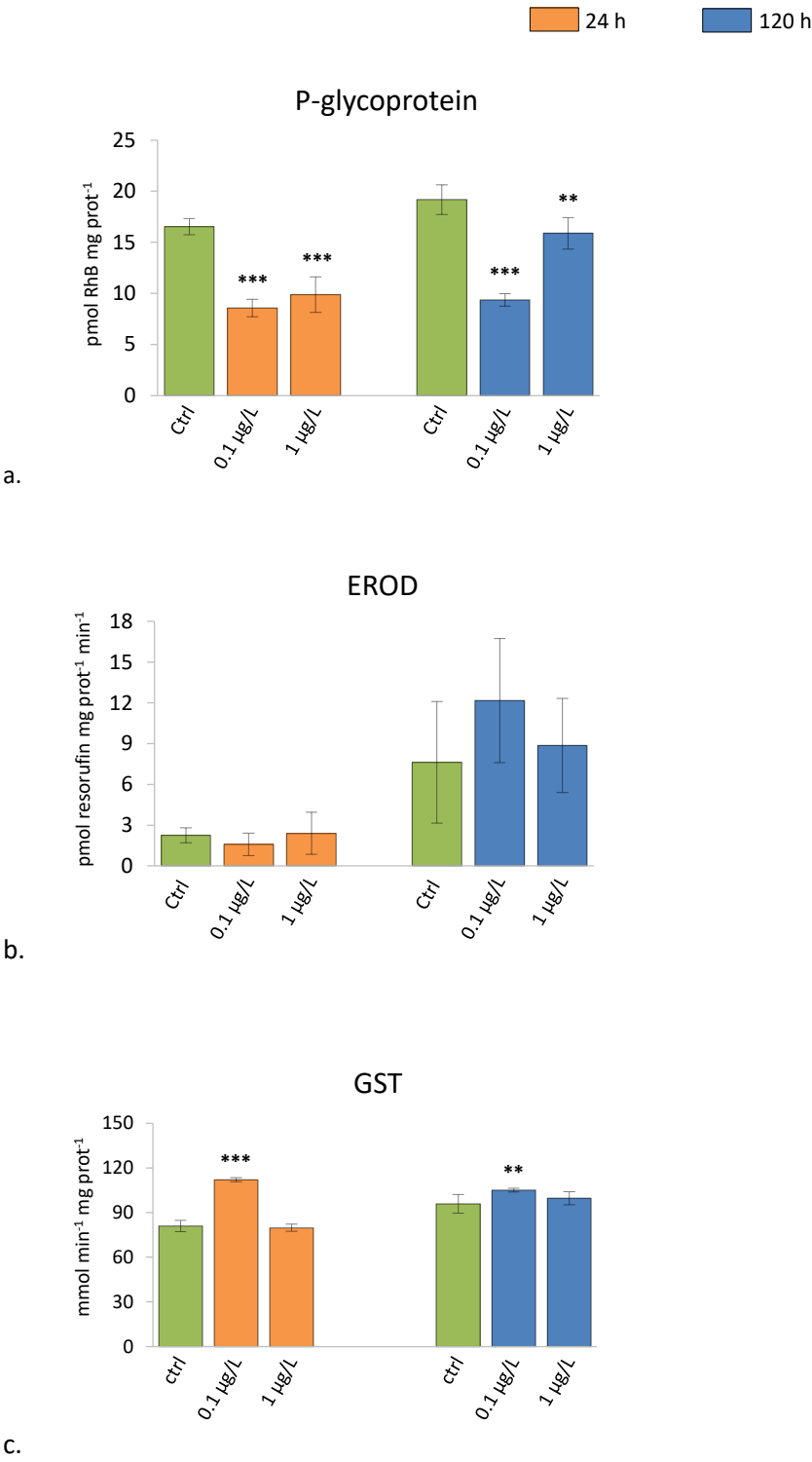
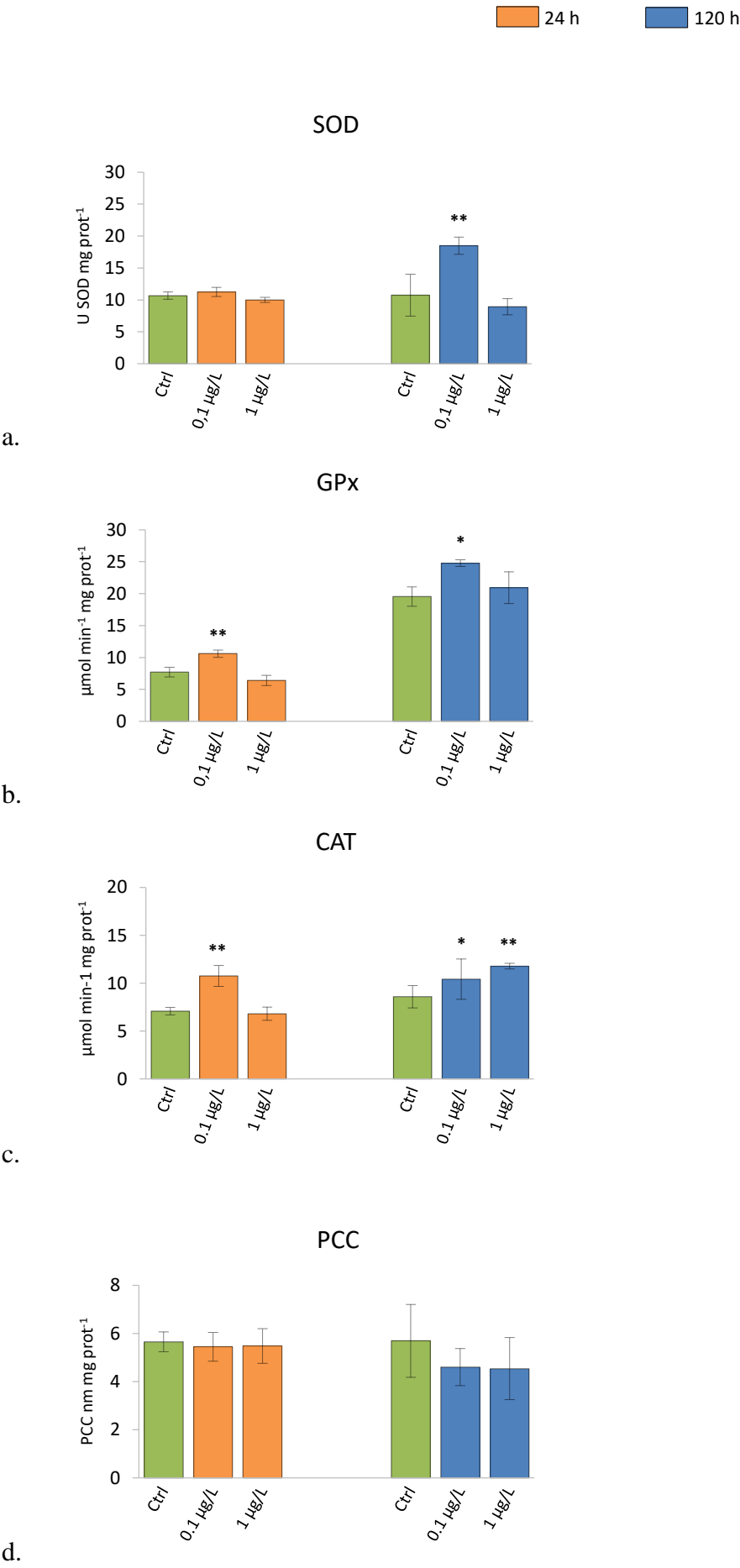
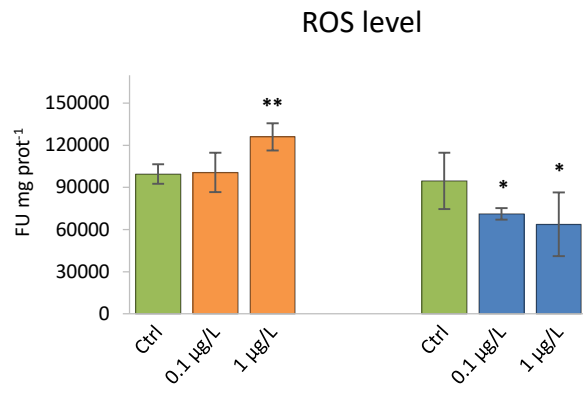


Figure
Click here to download Figure: Fig. 2.pdf





e.